Author Manuscript

Author Manuscript

Author Manuscript

Author Manuscript

HHS Public Access

Author manuscript

Curr Biol. Author manuscript; available in PMC 2019 March 05.

Published in final edited form as:

Curr Biol. 2018 March 05; 28(5): 817–823.e3. doi:10.1016/j.cub.2018.01.077.

Drosophila Full-Length Amyloid Precursor Protein is Required for Visual Working Memory and Prevents Age-Related Memory Impairment

Franziska Rieche[1], **Katia Carmine-Simmen**[2,3], **Burkhard Poeck**[1], **Doris Kretzschmar**[2,*], and **Roland Strauss**[1,4,*]

[1]Institut für Entwicklungsbiologie und Neurobiologie, Johannes Gutenberg-Universität Mainz, Colonel-Kleinmann-Weg 2, 55099 Mainz, Germany

[2]Oregon Institute of Occupational Health Sciences, 3181 S.W. Sam Jackson Park Rd. Portland, Oregon 97201-3098, USA

Summary

The β-amyloid precursor protein (APP) plays a central role in the etiology of Alzheimer's disease (AD). However, its normal physiological functions are still unclear. APP is cleaved by various secretases whereby sequential processing by the β- and γ-secretases produces the β-amyloid peptide that is accumulating in plaques that typify AD. In addition, this produces secreted N-terminal sAPPβ fragments and the APP intracellular domain (AICD). Alternative cleavage by α-secretase results in slightly longer secreted sAPPα fragments and the identical AICD. Whereas the AICD has been connected with transcriptional regulation, sAPPα fragments have been suggested to have a neurotrophic and neuro-protective role [1]. Moreover, expression of sAPPα in APP-deficient mice could rescue their deficits in learning, spatial memory, and long-term potentiation [2]. Loss of the *Drosophila* APPL (APP-Like) protein impairs associative olfactory memory formation and middle-term memory that can be rescued with a secreted APPL fragment [3]. We now show that APPL is also essential for visual working memory. Interestingly, this short-term memory declines rapidly with age and this is accompanied by enhanced processing of APPL in aged flies. Furthermore, reducing secretase-mediated proteolytic processing of APPL can prevent the age-related memory loss whereas overexpression of the secretases aggravates the aging effect.

[*]Correspondence: rstrauss@uni-mainz.de (R.S.) kretzsch@ohsu.edu (D.K.).

[3]Present Address: Department of Oncology, University of Alberta, Katz Group Centre, 114th Street and 87th Avenue, Edmonton, Alberta T6G 2E1, Canada

[4]Lead Contact

Supplemental Information

Supplemental information includes four figures and four data files comprising all statistical data.

Author Contributions

K.C.-S. and D.K. established the double-tagged APP/L transgene. F.R. and B.P. designed and carried out the behavioral and histological experiments, F.R. analyzed the data. D.K. performed the Western blot analysis. B.P., D.K., and R.S. conceived the project and wrote the manuscript.

Declaration of Interests

The authors declare no competing interests.

Publisher's Disclaimer: This is a PDF file of an unedited manuscript that has been accepted for publication. As a service to our customers we are providing this early version of the manuscript. The manuscript will undergo copyediting, typesetting, and review of the resulting proof before it is published in its final citable form. Please note that during the production process errors may be discovered which could affect the content, and all legal disclaimers that apply to the journal pertain.

Author Manuscript Author Manuscript Author Manuscript Author Manuscript

Rescue experiments confirmed that this memory requires signaling of full-length APPL and that APPL negatively regulates the neuronal-adhesion molecule Fasciclin 2. Overexpression of APPL or one of its secreted N-termini results in a dominant-negative interaction with the FASII receptor. Therefore, our results show that specific memory processes require distinct APPL products.

eTOC Blurb/In Brief

Walking flies can memorize the path to a vanished landmark for about 4s by integrating visual and idiothetic information about their own movements. Rieche *et al.* show that this memory is rapidly deteriorating with age and depends on Amyloid Precursor Protein-Like (APPL) signaling. Reducing cleavage of APPL ameliorates age-related memory deficits.

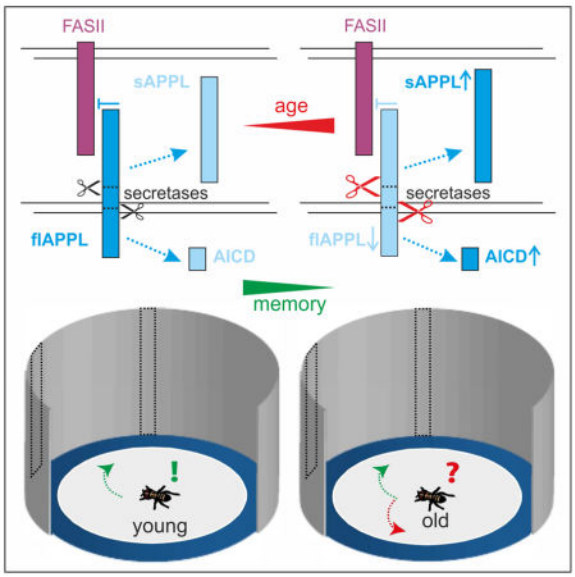

Keywords

age-related memory impairment; *Drosophila*; working memory; Amyloid Precursor Protein; visual orientation

Results and Discussion

Age-related memory impairment (AMI) affects all animals [4] and cognitive decline is one of the devastating features of Alzheimer's disease (AD) [5]. Although APP, and more specifically the β-amyloid peptide, have been connected with memory deficits in AD, the role of full-length APP and its various other fragments in AMI is unknown. Wild-type *Drosophila* flies display AMI at middle age (30–40d) when tested for middle-term [6] or long-term olfactory memory [7]. Furthermore, *Drosophila* not only encodes an orthologue for APP, called Amyloid Precursor Protein-like (APPL), but also homologues for all three types of secretases; *kuzbanian* (*kuz*) corresponds to ADAM10 considered to be an α-secretase, *dBace*, the fly β-secretase, and *Presenilin* (*Psn*), the catalytic subunit of γ-secretase. APPL is processed in a similar way as human APP [8], however, the cleavage sites of the α- and β-secretase are reversed [9]. Therefore, cleavage by KUZ produces a shorter

Author Manuscript Author Manuscript Author Manuscript Author Manuscript

secreted N-terminal fragment (NTF) than processing by dBACE. Nevertheless, subsequent γ-processing of the β-cleaved C-terminal fragment (βCTF) results in a neurotoxic dAβ-peptide, whereas cleavage by KUZ does not [8]. Here we asked whether the very short-term (~4s) visual working memory in flies [10] is also affected by AMI and whether it requires APPL or one of its proteolytic fragments. Therefore, we aged wild-type flies and heterozygous mutants for the three secretases and assessed their visual orientation memory.

Visual Working Memory Requires Full-length APPL in R3 Ring Neurons

This working memory is tested in the *detour* paradigm [10] where walking flies navigate between two inaccessible landmarks. During an approach, the targeted landmark disappears and the fly is lured towards a novel distracting landmark. This distracter disappears one second after reorientation so that the fly is now left without any landmarks (Figure S1). Nevertheless, wild-type Canton-S (CS) flies can recall the position of the initial landmark and try to approach it although still invisible ("positive choices" in following figures). Whereas young CS males make about 80% positive choices, aged flies showed a reduced memory when tested at 4 weeks of age and a complete memory loss when 6 weeks old (Figure 1A). Interestingly, heterozygosity for any of the three secretases prevented AMI, with 4- and 6–weeks-old Psn^{143}/+ and $kuz^{e29\text{-}4}$/+ flies being indistinguishable from young CS flies. When using heterozygous $dBace^{5243}$ flies, the improvement compared to age-matched CS controls did not reach significance; however they made significantly more positive choices than chance level at 6 weeks, whereas CS did not (Figure 1A). These findings show that visual working memory is deteriorating with age and they suggest that reducing APPL processing can suppress AMI.

To address whether increased processing of APPL disrupts this memory, we overexpressed the secretases in the R3 ring neurons of the ellipsoid body (using *189Y*-GAL4) the seat of visual working memory (for details about the neuronal circuit see Figure S1) [10, 11]. As shown in Figure 1B, expression of any of the secretases reduced the performance already in 3-days-old flies compared to controls, supporting a requirement of full-length flAPPL for this type of memory. On the other hand Western blot analyses using an antiserum directed against the NTFs of APPL (Ab952M [12]) established that heterozygous secretase mutants have an overall increase especially in flAPPL (Figure 1C) which supported our hypothesis on the role of secretases and APPL processing in AMI. Furthermore, a quantitative analysis of the levels of APPL in head extracts from different ages revealed that flAPPL declines with age whereas the NTF/flAPPL ratio increases (Figure 1D), also suggesting that reduced levels of flAPPL are involved in AMI. To verify that APPL is indeed required for visual working memory, we also tested homozygous $Appl^{d}$ null-mutants [13] and transheterozygous combinations of hypomorphic *Appl* alleles [14]. All these mutants performed at chance level already when young, confirming that APPL is necessary for this short-termed memory (Figure 1E). This function is dose-sensitive because even young heterozygous $Appl^{d}$/+ showed a reduced memory that declined faster with age than in CS females (Figure 1F).

Next we induced an RNA interference (RNAi [15]) mediated knockdown of *Appl* in the R3 neurons which resulted in severe memory deficits already in 3–5 days-old flies, showing that

Author Manuscript Author Manuscript Author Manuscript Author Manuscript

APPL is required in these neurons for visual working memory (Figure S2). To identify domains in APPL that mediate this function, we performed rescue experiments expressing different APPL constructs via *189Y*-GAL4 in young $Appl^{d}$ mutant flies (Figure 2). This included full-length flAPPL, secretion-defective sdAPPL, specific deletion constructs, and secreted fragments (Figure 2D) [16]. Because the exact cleavage sites in APPL are unknown, we refer to the secreted fragments as $sAPPL^{Long\ (L)}$, which comprises the N-terminal 788 amino acids [16] and should represent the β-cleaved fragment, whereas the 758aa long $sAPPL^{Short\ (S)}$ should represent the α-cleaved form of *Drosophila* APPL [17]. In contrast to full-length wild-type APPL, neither of the secreted forms could rescue the memory deficit of $Appl^{d}$ when induced in R3 neurons ($sAPPL^{L}$ and $sAPPL^{S}$ in Figure 2A). Notably, sdAPPL very effectively rescued the memory phenotype, confirming that unprocessed flAPPL is crucial for visual working memory.

Secretion-defective sdAPPL Acts as a Ligand and Prevents Age-Related Memory Impairment (AMI)

Next, we investigated whether APPL functions as a receptor or ligand in R3 neurons. Expression of sdAPPL that in addition lacks the intracellular C-terminus (sdAPPL-ΔC [16]) did rescue the $Appl^{d}$ memory phenotype, which suggests that intracellular signaling is not required and that APPL does not act as a receptor. Rescue experiment with sdAPPL forms that, in addition, lack one of the two ectodomains (sdAPPL-ΔE1 and sdAPPL-ΔE2 [16]), revealed a requirement for E2 for the rescue but not for E1 (Figure 2A). To confirm this, we repeated the rescue experiment with the hypomorphic $Appl^{4460}$ allele and APPL, sdAPPL, and sdAPPL-ΔE1 rescued to full extent, whereas sdAPPL-ΔE2 did not (Figure S2). These results suggest that membrane-bound APPL functions as a ligand in the ring neurons. This function was conserved in human APP because expression of APP_{695} via *189Y*-GAL4 in $Appl^{d}$ also resulted in a rescue (Figure S2). Using conditional expression of APPL (by combining *189Y*-GAL4 with the temperature-sensitive GAL4 repressor *Tub*>$GAL80^{ts}$ [18]) resulted in the same rescue as constitutive expression, revealing that expression in adult R3 neurons is sufficient to restore the memory in 3–5 days-old flies (Figure 2B). Notably, using the same expression system to induce moderate overexpression of sdAPPL (at 25°C), we were able to rescue the AMI in a wild-type background (Figure 2C) demonstrating that the secretion-deficient unprocessed APPL can prevent the decline of visual working memory of aged flies. Together with the finding that the levels of endogenous flAPPL decrease with age (Figure 1D), this suggests that a loss of flAPPL underlies the visual working memory deficits that occur during normal aging. Interestingly, an age-related increase in BACE1 activity has been described in vertebrates [19] that could reduce levels of full-length APP.

Most of APPL functions in synaptogenesis, neurite outgrowth and guidance described so far required signaling via the C-terminal domain [9, 20]. Analyzing heterozygous $Appl^{d}/+$ mutant flies or inducing an adult-specific knockdown of *Appl* in the relevant mushroom body neurons, Preat and Goguel showed that APPL function is not required for olfactory learning, but for a 2h associative memory and long-term memory formation [21]. Similar to findings in mice, overexpression of secreted $sAPPL^{L}$ (as well as APPL and sdAPPL) could restore the 2h memory in heterozygous $Appl^{d}/+$ flies, whereas only wild-type APPL could

Author Manuscript Author Manuscript Author Manuscript Author Manuscript

rescue the long-term memory deficit. Because endogenous APPL was still expressed in this rescue experiments, $sAPPL^{L}$ and sdAPPL might act as ligands that bind to flAPPL in mushroom body neurons. The authors therefore suggested that distinct memory phases require different forms of APPL and maybe different intracellular signaling pathways [3, 21]. Notably, overexpression of KUZ in the mushroom body did not affect the 2h olfactory memory [21], whereas KUZ in our study significantly reduced visual working memory. It should also be noted that unprocessed APPL can be deleterious, because expression of sdAPPL in photoreceptor cells caused cell-death of lamina glia via an unknown receptor [22]; further emphasizing that individual neuronal networks may require different APPL fragments and signaling pathways.

Due to recent studies suggesting that output from the R3 neurons into the ellipsoid body is instrumental for visual working memory [11] we hypothesized that full-length APPL is present at the axonal terminals of R3 neurons in the ellipsoid body. To analyze the sub-cellular localization of APPL and its fragments, we used a double-tagged version of APPL (dtAPPL) [23] that carries an EGFP-tag near the N-terminus and RFP-tag at the C-terminus (Fig. S3C), resulting in yellow fluorescence of full-length dtAPPL (or co-localized fragments that have not been separated yet). Using *189Y*-GAL4 to induce dtAPPL, we observed that dtAPPL is processed differently in individual R3 neurons (Figures 3A–3D), whereby full-length as well as fragments of dtAPPL are found in the cell bodies and axonal/dendritic projections (Figures 3B–3D). That significant amounts of unprocessed APPL can be found in the R3 axons in the ellipsoid body (Figure 3D) supports the model, that full-length APPL is needed at the R3 output sites. Note that dtAPPL was able to rescue the memory deficit, as did a $dtAPP_{695}$ which showed a similar distribution pattern as dtAPPL (Figure S3).

Having established that full-length APPL can be found at the relevant output sides, we asked whether proteolytic processing of APPL also changes in the R3 neurons with age. Comparing the pattern of $dtAPP_{695}$ expressed with the *189Y*-GAL4 driver in 3d- and 6-week-old flies indicated less full-length $dtAPP_{695}$ in aged flies, but when quantifying this, it did not reach significance ($p = 0.064$; Figure S3). Therefore, we used another R3-neuron-specific GAL4 line (VT42759 [24]) that results in reduced levels of $dtAPP_{695}$ with increasing age (Figures 3E–3G), but could nevertheless be used to rescue the memory phenotype of $Appl^{d}$ (Figure S3). Compared to 3d-old flies there was little co-localization of GFP tagged N-termini and RFP tagged C-termini in 6-week-old VT42759>dtAPP flies (Pearson's correlation coefficient: 3 days PCC = 0.8855, n = 6 vs. 6 weeks PCC = 0.078, n = 5 and $p = 0.006$; see Figure S3), revealing enhanced proteolytic processing of APP. This suggests that AMI of the visual orientation memory is caused by increased ectodomain shedding of APPL and Western blot analysis of aged flies supports this notion because during aging the ratio of NTFs to flAPPL increases (Figure 1D).

Author Manuscript Author Manuscript Author Manuscript Author Manuscript

APPL Inhibits the Function of the NCAM140 Homolog FASII in R3 Ring Neurons

To identify a possible receptor for APPL in visual working memory, we focused on the neural cell adhesion molecule Fasciclin 2 (FASII). FASII is enriched in most, if not all types [25, 26] of ring neurons in the ellipsoid body (Figure S4) and it has been shown to interact with APPL in synaptic bouton formation at the neuromuscular junction (NMJ) [27]. Moreover, FASII is the insect homolog of NCAM-140, which has been demonstrated to bind APP in an E2-depending fashion [28]. When we tested young hemizygous mutants for the strong hypomorphic *FasII*^{e76} allele [14] in the detour paradigm, they showed no working memory (Figure 4A) and the same phenotype was observed when we induced an RNAi [29] against *FasII* in R3 neurons of 3–5 days-old flies (Figure 4B, the knockdown was confirmed by immunohistochemistry Figure 4C–4D). This phenotype could be rescued by expression of FASII [30] in R3 neurons, which reveals that FASII is required in the same ring neuron subtype as APPL, providing a possible binding partner for APPL (Figure 4A). At the NMJ, loss of APPL suppressed the increase in bouton number in heterozygous *FasII*^{e76}/+ larvae [27]. We therefore investigated whether removing one copy of *Appl* could rescue the memory deficits of homozygous *FasII*^{e76} mutants. As shown in Figure 4E, this resulted in a significant improvement in performance, as did one copy of the *FasII*^{e76} mutant allele in homozygous *Appl*^{d} null-mutant flies. Moreover, reducing FASII expression in R3 neurons by RNAi also ameliorated the memory deficit of *Appl*^{d} null-mutants (Figure 4F). Together this suggests that APPL negatively regulates FASII in R3 neurons and that FASII acts downstream of APPL. That this negative interaction is essential to prevent AMI is demonstrated by the observation that heterozygosity for *FasII*^{e76} suppresses the memory loss of 4-week-old heterozygous *Appl*^{d}/+ flies (Figure S4).

To further investigate interactions between APPL and FASII, we performed over-expression studies using young flies and found that elevated levels of flAPPL or sdAPPL ameliorated the memory deficit induced by FASII overexpression (Figures 4G and 4H). However, only wild-type APPL induced memory deficits when overexpressed without FASII. This suggested that a secreted form of APPL can induce a gain-of-function phenotype and we therefore overexpressed sAPPL^{L} and sAPPL^{S} in R3 neurons. Whereas sAPPL^{L} had no effect (Figure 4I), sAPPL^{S} caused a severe impairment of visual working memory (Figure 4J). Moreover, overexpression of sAPPL^{S} suppressed the effects of elevated FASII levels, whereas sAPPL^{L} did not. This shows that sAPPL^{S}, which corresponds to the α-cleaved (KUZ) fragment, has deleterious effects when overexpressed and that these are also mediated by an interaction with FASII. Whether the lack of an effect of sAPPL^{L} overexpression is due to a less efficient interaction with FASII or an inability to induce downstream pathways causing this gain-of function remains to be determined.

Interestingly, overexpression of the dAICD [17] in R3 neurons also disrupted visual working memory of young flies (Figure S2), suggesting that α- and γ-cleavage of APPL has deleterious effects on visual working memory. This is in agreement with our finding that heterozygosity for *kuz* and *Psn* ameliorated the age-related decline in visual working memory whereas heterozygosity for dBACE had only a modest effect. This could be

Author Manuscript Author Manuscript Author Manuscript Author Manuscript

explained by assuming that most of the ectodomain shedding in flies is done by KUZ activity. Therefore reducing dBACE levels might result in a small increase of flAPPL. In addition competitive KUZ cleavage in *dBace*/+ flies could result in more detrimental $sAPPL^S$. Whereas in the case of *kuz/+*, the effects on memory are mediated by the interaction with FASII, in the case of *Psn/+* this may be mediated by a transcriptional function of the AICD [1], affecting a so far unknown target.

Conclusion

In summary, our results show that full-length APPL acts as a membrane-bound ligand that inhibits the FASII receptor (both acting in R3 neurons), thereby promoting visual working memory. Increased proteolytic APPL processing and therefore reduced suppression of FASII signaling then seems to cause AMI in flies. A similar interaction might also be required for working memories in vertebrates. Aging mice show reduced expression of NCAM-140 in the medial prefrontal cortex and a conditional knock-out of NCAM in the forebrain promotes AMI in a delayed matching-to-place test in the Morris water maze and in a delayed reinforced alternation test in the T-maze [31].

STAR*Methods

CONTACT FOR REAGENT AND RESOURCE SHARING

Further information and requests for resources and reagents should be directed to and will be fulfilled by the Lead Contact, Roland Strauss (rstrauss@uni-mainz.de).

EXPERIMENTAL MODEL AND SUBJECT DETAILS

Drosophila melanogaster strains were maintained on standard medium (water, cornmeal, malt extract, molasses, yeast, soy bean, agar, preservative methyl-4-hydroxybenzoate) at 25°C, 60% humidity, and 14h/10h light-dark cycles. For aging newly hatched flies were separated by gender and transferred to a new vial on every 3rd day. Male flies were used in all experiments, except when heterozygous *Appl* mutants were studied. The $Appl^d$ $FasII^{e76}$ chromosome was established by meiotic recombination of $Appl^d$ *w** with $FasII^{e76}$. All mutant lines were brought into a wild-type Canton S background, WT-CS was used to generate heterozygous flies and CS was used as a control in all experiments. For adult specific rescue experiments using the *Tub*-$GAL80^{ts}$ transgene, crosses were maintained and the progeny were raised at 18°C. After eclosion, flies were selected at 4°C, their wings s hortened and returned to 18°C for behavioral experiments on the following day. After 15min recovery at room temperature, flies were tested in the detour paradigm. To induce GAL4 activity, the same flies were incubated at 30°C overnight and tested again after a 15min recovery period. The 189Y-GAL4 *Tub*>$GAL80^{ts}$ line was stablished by meiotic recombination [11]. For mild overexpression of sdAPPL in aging flies *189Y*-GAL4 *Tub*>$GAL80^{ts}$/UAS-sdAPPL and control flies were raised and aged at 25°C.

METHOD DETAILS

Behavioral analysis—Flies with their wings cut to one third of their length under cold anesthesia (one day before testing) were analyzed in an LED arena that has been described

Author Manuscript Author Manuscript Author Manuscript Author Manuscript

in Neuser *et al.* [10]; see also Figure S1. Individual flies were tested 10 times for positive choices, i.e. orientation towards the position of the vanished landmark.

Immunohistochemistry—Immunohistochemistry was performed as described in the Fly Light Project Immunohistochemistry protocol [34], modifying some steps. Brains were dissected in *Drosophila* Ringer' solution (3mM $CaCl_2$•2H2O, 182mM KCl, 46mM NaCl, 10mM Tris, pH 7.2) and fixed in 1% para-formaldehyde/Ringer's solution over night at 4°C. All following washes and incubations were done in PAT-3 (0.5% Triton X-100, 0.5% Bovine Serum Albumin, PBS). 3% horse or goat serum was added for blocking cross reactivity for 90min at RT. Primary antibodies were used at the following dilutions in 3% horse/goat serum PAT-3 for sequential incubation at RT (3 hours) and 4°C overnight: anti-FASII 1:100 (mouse); anti-GFP 1:1000 (chicken); anti-RFP 1:1000 (mouse). For visualization of the double-tagged APPL and APP, fluorescent labeled primary antibodies were used: anti-GFP-Alexa-488 1:100 (rabbit); anti-RFP-CF594 1:200 (rabbit). All secondary antibodies were diluted 1:1000 in 3% horse/goat serum/PAT-3. The secondary antibody was diluted in blocking buffer and incubations done for 1–3 hours at room temperature before transferring to 4°C for 4–5 days following mounting in Vectashield. Images were acquired using a laser scanning microscope (Leica TCS SP8) and the Leica LASX software.

Western blot analysis—Adult fly heads were dissected on a cold plate, homogenized in Tris-glycine SDS loading buffer containing protease inhibitor, and allowed to incubate at room temperature for 45 minutes. TCEP (tris[2-carboxyethyl]phosphine) was used to reduce samples at 75°C for 10 minutes, followed by centrifugation at 10,000 x g for 15 minutes. The supernatant was denatured at 75°C for an additional 10 minutes and the equivalent of 2 heads per lane loaded on 3–8% gradient SDS-PAGE gels. Following transfer to a polyvinylidene fluoride (PVDF) membrane, the blots were washed with Tris-buffered saline plus 0.1% Tween-20 (TBST) and blocked with TBST/casein blocking buffer. Membranes were then incubated with rabbit anti-APPL serum (1:4000; a gift by K. White, Brandeis University) and mouse anti-GAPDH (1:250) at 4°C overnight. Secondary HRP-conjugated goat anti-rabbit and HRP-conjugated goat anti-mouse antibodies (1:10,000) were used at room temperature for 2–4h. Proteins were detected with enhanced Chemiluminescence DuoLuX. The ratios of pixel intensities were analyzed with Fiji [33].

QUANTIFICATION AND STATISTICAL ANALYSIS

Quantification of fluorescence signals—For quantitative expression assessments of the FASII knock-out, samples were scanned with identical settings and analyzed with Fiji [33]. For measurements of FASII expression in the R3 neurons, a 7 x 3 μm rectangular region of interest was selected on the basis of the strongest *189Y*-GAL4>mCD8::GFP expression and a stack of 3 μm thickness created. For a reference, an equally-sized rectangular region (z = 3 μm) was drawn in the area of the surrounding R2-neuron innervation site in the ellipsoid body. Within a region of interest, the grey values of all pixels with a common x-/y-coordinate were summed up along the z-axis (creating voxels), the mean of all voxels was determined, and quotients of the R3/R2 intensities were calculated.

Author Manuscript Author Manuscript Author Manuscript Author Manuscript

For co-localization analysis, images were first subjected to a deconvolution using the Huygens software and a theoretical point spread function (PSF) created by the software using the given image details and microscope settings. After the deconvolution, all optical sections displaying anti-GFP and anti-RFP immunoreactivity in the ellipsoid body were stacked. The Pearson's correlation coefficient (PCC) was calculated using the Huygens software with an automated threshold setting (Costes automatic threshold method). PCC is a measure of the linear correlation between two variables (green and red fluorescent pixels). PCC is the covariance of the two variables divided by the product of their standard deviations. Values can range from 1 for two images whose fluorescence intensities are perfectly linearly related, to −1 for two images whose fluorescence intensities are inversely related to one another.

Statistical analysis—Statistical analyses were performed with STATISTICA 8.0 (α level 0.05 in all cases). Single sample t-test or Sign test was used to compare against the chance level of 58%. Kruskal-Wallis test was used for multiple comparisons, applying post Bonferroni hoc. Significance is indicated in all figures by: (n.s.) not significant; (*) $P<0.05$; (**) $P<0.01$; (***) $P<0.001$.

DATA AND SOFTWARE AVAILABILITY

Data—Detailed statistical analyses for all behavioral experiments are given in Data S1–S4.

Supplementary Material

Refer to Web version on PubMed Central for supplementary material.

Acknowledgments

We like to thank V. Buddnik, M. Fortini, S Goode, and L. Torroja, for contributing valuable fly lines. We are also grateful to K. White who shared the anti-APPL serum. Additional lines were obtained from the Bloomington *Drosophila* Stock Center (BDSC; NIH P40OD018537), Vienna *Drosophila* Research Center (VDRC), and the Exelixis stock collection (Harvard). We like to thank Alexander Law for technical assistance. The study was funded by the Deutsche Forschungsgemeinschaft STR 590/5-1 (BP&RS), STR 590/6-1 (RS) and NIH grant R01 AG045830 (DK).

References

1. Nhan HS, Chiang K, Koo EH. The multifaceted nature of amyloid precursor protein and its proteolytic fragments: friends and foes. Acta Neuropathol. 2015; 129:1–19. [PubMed: 25287911]
2. Aydin D, Weyer SW, Muller UC. Functions of the APP gene family in the nervous system: insights from mouse models. Exp Brain Res. 2012; 217:423–434. [PubMed: 21931985]
3. Preat T, Goguel V. Role of *Drosophila* Amyloid Precursor Protein in Memory Formation. Front Mol Neurosci. 2016; 9:142. [PubMed: 28008309]
4. Bishop NA, Lu T, Yankner BA. Neural mechanisms of ageing and cognitive decline. Nature. 2010; 464:529–535. [PubMed: 20336135]
5. Scheltens P, Blennow K, Breteler MM, de Strooper B, Frisoni GB, Salloway S, Van der Flier WM. Alzheimer's disease. Lancet. 2016; 388:505–517. [PubMed: 26921134]
6. Yamazaki D, Horiuchi J, Nakagami Y, Nagano S, Tamura T, Saitoe M. The *Drosophila* DCO mutation suppresses age-related memory impairment without affecting lifespan. Nat Neurosci. 2007; 10:478–484. [PubMed: 17322874]

Author Manuscript Author Manuscript Author Manuscript Author Manuscript

7. Mery F. Aging and its differential effects on consolidated memory forms in *Drosophila*. Exp Gerontol. 2007; 42:99–101. [PubMed: 16860960]
8. Carmine-Simmen K, Proctor T, Tschape J, Poeck B, Triphan T, Strauss R, Kretzschmar D. Neurotoxic effects induced by the *Drosophila* amyloid-beta peptide suggest a conserved toxic function. Neurobiol Dis. 2009; 33:274–281. [PubMed: 19049874]
9. Poeck B, Strauss R, Kretzschmar D. Analysis of amyloid precursor protein function in *Drosophila melanogaster*. Exp Brain Res. 2012; 217:413–421. [PubMed: 21912928]
10. Neuser K, Triphan T, Mronz M, Poeck B, Strauss R. Analysis of a spatial orientation memory in *Drosophila*. Nature. 2008; 453:1244–1247. [PubMed: 18509336]
11. Kuntz S, Poeck B, Strauss R. Visual Working Memory Requires Permissive and Instructive NO/cGMP Signaling at Presynapses in the *Drosophila* Central Brain. Curr Biol. 2017; 27:613–623. [PubMed: 28216314]
12. Torroja L, Luo L, White K. APPL, the *Drosophila* member of the APP-family, exhibits differential trafficking and processing in CNS neurons. J Neurosci. 1996; 16:4638–4650. [PubMed: 8764652]
13. Luo L, Tully T, White K. Human amyloid precursor protein ameliorates behavioral deficit of flies deleted for *Appl* gene. Neuron. 1992; 9:595–605. [PubMed: 1389179]
14. Gramates LS, Marygold SJ, Santos Gd, Urbano JM, Antonazzo G, Matthews BB, Rey AJ, Tabone CJ, Crosby MA, Emmert DB, et al. FlyBase at 25: looking to the future. Nucl Acids Res. 2016; 45:D663–D671. [PubMed: 27799470]
15. Ni JQ, Liu LP, Binari R, Hardy R, Shim HS, Cavallaro A, Booker M, Pfeiffer BD, Markstein M, Wang H, et al. A *Drosophila* resource of transgenic RNAi lines for neurogenetics. Genetics. 2009; 182:1089–1100. [PubMed: 19487563]
16. Torroja L, Packard M, Gorczyca M, White K, Budnik V. The *Drosophila* beta-amyloid precursor protein homolog promotes synapse differentiation at the neuromuscular junction. J Neurosci. 1999; 19:7793–7803. [PubMed: 10479682]
17. Wentzell JS, Bolkan BJ, Carmine-Simmen K, Swanson TL, Musashe DT, Kretzschmar D. Amyloid precursor proteins are protective in *Drosophila* models of progressive neurodegeneration. Neurobiol Dis. 2012; 46:78–87. [PubMed: 22266106]
18. McGuire SE, Le PT, Osborn AJ, Matsumoto K, Davis RL. Spatiotemporal rescue of memory dysfunction in *Drosophila*. Science. 2003; 302:1765–1768. [PubMed: 14657498]
19. Fukumoto H, Rosene DL, Moss MB, Raju S, Hyman BT, Irizarry MC. Beta-secretase activity increases with aging in human, monkey, and mouse brain. Am J Pathol. 2004; 164:719–725. [PubMed: 14742275]
20. Nicolas M, Hassan BA. Amyloid precursor protein and neural development. Development. 2014; 141:2543–2548. [PubMed: 24961795]
21. Bourdet I, Preat T, Goguel V. The full-length form of the *Drosophila* amyloid precursor protein is involved in memory formation. J Neurosci. 2015; 35:1043–1051. [PubMed: 25609621]
22. Bolkan BJ, Triphan T, Kretzschmar D. beta-secretase cleavage of the fly amyloid precursor protein is required for glial survival. J Neurosci. 2012; 32:16181–16192. [PubMed: 23152602]
23. Ramaker JM, Cargill RS, Swanson TL, Quirindongo H, Cassar M, Kretzschmar D, Copenhaver PF. Amyloid Precursor Proteins Are Dynamically Trafficked and Processed during Neuronal Development. Front Mol Neurosci. 2016; 9:130. [PubMed: 27932950]
24. Lin CY, Chuang CC, Hua TE, Chen CC, Dickson BJ, Greenspan RJ, Chiang AS. A comprehensive wiring diagram of the protocerebral bridge for visual information processing in the *Drosophila* brain. Cell Rep. 2013; 3:1739–1753. [PubMed: 23707064]
25. Young JM, Armstrong JD. Structure of the adult central complex in *Drosophila*: organization of distinct neuronal subsets. J Comp Neurol. 2010; 518:1500–1524. [PubMed: 20187142]
26. Martin-Pena A, Acebes A, Rodriguez JR, Chevalier V, Casas-Tinto S, Triphan T, Strauss R, Ferrus A. Cell types and coincident synapses in the ellipsoid body of *Drosophila*. Eur J Neurosci. 2014; 39:1586–1601. [PubMed: 24605774]
27. Ashley J, Packard M, Ataman B, Budnik V. Fasciclin II signals new synapse formation through amyloid precursor protein and the scaffolding protein dX11/Mint. J Neurosci. 2005; 25:5943–5955. [PubMed: 15976083]

Author Manuscript Author Manuscript Author Manuscript Author Manuscript

28. Chen KP, Dou F. Selective interaction of amyloid precursor protein with different isoforms of neural cell adhesion molecule. J Mol Neurosci. 2012; 46:203–209. [PubMed: 21691800]

29. Dietzl G, Chen D, Schnorrer F, Su KC, Barinova Y, Fellner M, Gasser B, Kinsey K, Oppel S, Scheiblauer S, et al. A genome-wide transgenic RNAi library for conditional gene inactivation in *Drosophila*. Nature. 2007; 448:151–156. [PubMed: 17625558]

30. Lin DM, Goodman CS. Ectopic and increased expression of Fasciclin II alters motoneuron growth cone guidance. Neuron. 1995; 13:507–523.

31. Bisaz R, Boadas-Vaello P, Genoux D, Sandi C. Age-related cognitive impairments in mice with a conditional ablation of the neural cell adhesion molecule. Learn Mem. 2013; 20:183–193. [PubMed: 23504516]

32. Ye Y, Fortini ME. Apoptotic activities of wild-type and Alzheimer's disease-related mutant presenilins in *Drosophila melanogaster*. J Cell Biol. 1999; 146:1351–1364. [PubMed: 10491396]

33. Schindelin J, Arganda-Carreras I, Frise E, Kaynig V, Longair M, Pietzsch T, Preibisch S, Rueden C, Saalfeld S, Schmid B, et al. Fiji: an open-source platform for biological-image analysis. Nat methods. 2012; 9:676–682. [PubMed: 22743772]

34. Jenett A, Rubin GM, Ngo TT, Shepherd D, Murphy C, Dionne H, Pfeiffer BD, Cavallaro A, Hall D, Jeter J, et al. A GAL4-driver line resource for *Drosophila* neurobiology. Cell Rep. 2012; 2:991–1001. [PubMed: 23063364]

Author Manuscript Author Manuscript Author Manuscript Author Manuscript

Highlights

- Visual working memory is particular sensitive to age-related memory impairment (AMI)
- Reducing secretase mediated processing of the *Drosophila* APP protein ameliorates AMI
- Levels of unprocessed full-length *Drosophila* APP protein are decreased in old flies
- Full-length *Drosophila* APP inhibits signaling by the neuronal-adhesion molecule FASII

Author Manuscript Author Manuscript Author Manuscript Author Manuscript

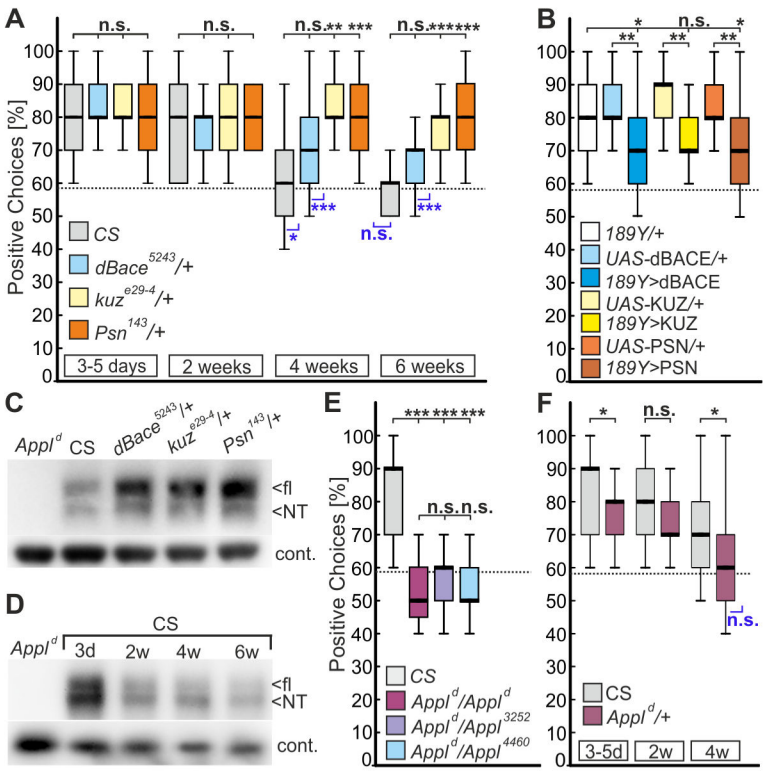

Figure 1. Reduced APPL processing promotes visual working memory in aged flies

(A) Wild-type CS and heterozygous mutants for the three secretases were aged for up to six weeks and tested for positive choices in the detour paradigm (n = 25 males for all groups). Whereas CS shows a reduced performance with age, heterozygosity for *kuz* or *Psn* prevents this decline.

(B) Overexpression of secretases (UAS-*kuz*, UAS-*dBace*, or UAS-*Psn*) in R3-neurons with *189Y*-GAL4 impairs the memory in 3-to-5-days-old flies compared to GAL4 and UAS-controls (n = 25 males).

(C) Western blot with head extracts from heterozygous secretase mutants (all 3-day old) show an increase in flAPPL using an antiserum against the N-terminus (NT) of APPL (Ab952M; [12]). *Appl*^{d} null-mutants were included as controls. A mouse monoclonal antibody against Glycerinaldehyd-3-Phosphat-Dehydrogenase (GAPDH) served as loading control.

(D) Western blot with anti-APPL and aged wild-type CS flies. Whereas the overall levels of APPL are increased in young (3d) CS flies compared to all other ages, the NTF/flAPPL ratio increases continuously with age (mean ratio 3d: 1.92 ± 0.125; 2w: 3.71 ± 0.35; 4w: 4.04 ± 0.63; 6w: 5.37 ± 1.08). The NTF/flAPPL ratio in 3d-old flies is significantly different from the ratio in aged flies: 3d/2w p = 0.0085; 3d/4w p = 0.0304; 3d/6w p = 0.0334 (n = 3). An unpaired t-test was used.

(E) Homozygous *Appl*^{d} null-mutants and transheterozygous mutants for hypomorphic *Appl* alleles show a complete loss of visual working memory (n = 16–25 females; age 3–5d).

(F) Heterozygous flies for the *Appl*^{d} null-mutant show a reduced orientation memory already when 3–5 days old that further declines with age (n = 25 females).

Author Manuscript Author Manuscript Author Manuscript Author Manuscript

Boxes always signify 25% and 75%-quartiles, thick lines medians and whiskers 10% and 90%-quantiles. The random choice level of 58% is shown by a dashed line. Significance to this chance level is indicated in blue below the boxes (non-parametric data, sign test; parametric data, one-sample t-test. n.s., not significant; *, $p<0.05$; **, $p<0.001$; ***, $p<0.001$). Shapiro-Wilk test for normal distribution; Kruskal-Wallis ANOVA, and Bonferroni post-hoc were used. See Data S1 for statistical analysis and Figure S1 for a schematic outline of the detour paradigm.

Author Manuscript Author Manuscript Author Manuscript Author Manuscript

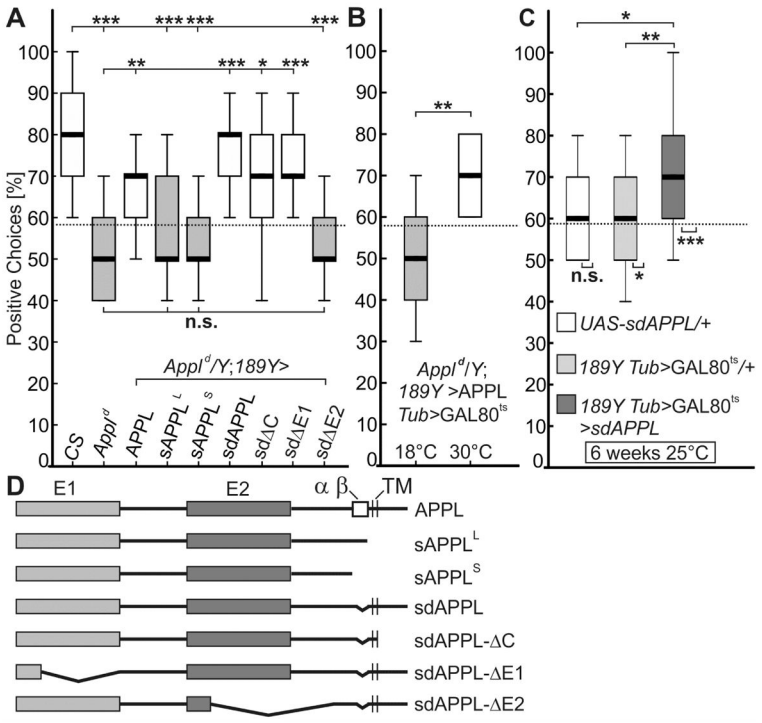

Figure 2. Membrane-bound full-length APPL is required for visual working memory

(A) Expression of wild-type APPL or secretion-defective sdAPPL in R3-neurons (*189Y*-GAL4) can rescue the memory deficit of *Appl*^{d} null-mutants. Ectodomain E2, but not E1, has to be present in sdAPPL to fulfil this function. The secreted fragments sAPPL^{S} and sAPPL^{L} are unable to rescue memory impairment in *Appl*^{d}. (n = 25 males; age 3–5d; n.s., not significant; *, p<0.05; **, p<0.001; ***, p<0.001; Kruskal-Wallis ANOVA, Bonferroni post-hoc).

(B) Conditional expression of APPL via *189Y*-GAL4 *Tub*>GAL80^{ts} (30°C incubation overnight) rescues the memory deficit compared to uninduced controls (18°C). The same flies were tested before and after temperature change. n = 14 males; **, p<0.001; Wilcoxon Matched Pairs test. See Figure S2 for evaluation of the APP$_{695}$ transgene and rescues of the hypomorphic *Appl*^{4460} allele.

(C) Limited overexpression of sdAPPL with the *189Y*-GAL4 *Tub*>GAL80^{ts} driver line at 25°C (n = 25) improved the memory deficit in comparison to aged-matched controls (UAS-sdAPPL/II, n = 15 and *189Y*-GAL4 *Tub*>GAL80^{ts}/II, n = 25; Kruskal-Wallis ANOVA, Bonferroni post-hoc). See Data S2 for statistical analysis.

(D) Schematic display of the APPL constructs used in the rescue experiment.

Author Manuscript Author Manuscript Author Manuscript Author Manuscript

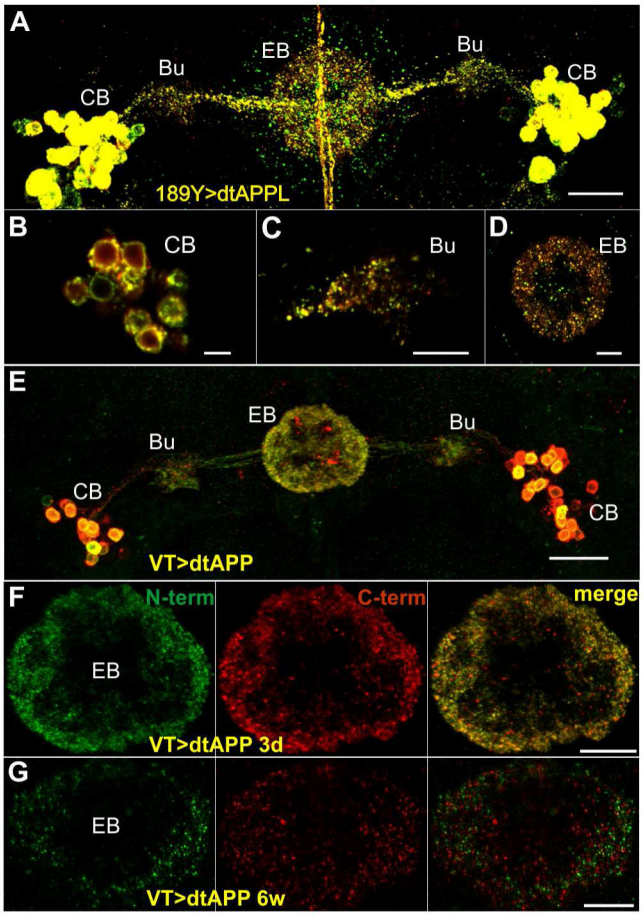

Figure 3. Cellular distribution of double-tagged APP/L and their fragments in R3 neurons

(A–D) Localization of dtAPPL and its proteolytic fragments in R3 neurons. (A) Overview of dtAPPL expression in R3 neurons (56.25 μm z-projection; scale bar 20 μm); cell bodies (CB) in the cortex, dendritic fields in the bulb (Bu), and axonal projections in the ellipsoid body (EB) are indicated.

(B) Individual R3 cell bodies show different APPL processing (300 nm z-projection; scale bar 5 μm).

(C) Most dtAPPL in the dendrites in the blub is cleaved (300 nm z-projection; scale bar 10 μm.

(D) CTF/dAICD (red), N-terminal fragments (green), as well as full-length dtAPPL (yellow) can be detected in the axons in the EB (300 nm z-projection; scale bar 10 μm).

(E–G) Localization of full-length dtAPP (yellow), N-terminal (green), and C-terminal (red) fragments produced from two copies of the dtAPP transgene driven with *VT45759*-GAL4.

(E) Overview of dtAPP expression in the R3-neurons (3-day old 48.75 μm z-projection; scale bar 20 μm). (F) In 3-day-old flies most of the fluorescent puncta in the axonal projections in the EB are yellow, indicating full-length APP or close proximity of cleaved fragments. (G) In contrast, reduced expression levels and minimal co-localization of the N- and C-termini can be observed in 6-week-old flies (3 μm z-projection; scale bar 10 μm). See

Author Manuscript Author Manuscript Author Manuscript Author Manuscript

Figure S3 for evaluation of the VT driver line and co-localization analysis (including *189Y* driven dtAPP).

Author Manuscript Author Manuscript Author Manuscript Author Manuscript

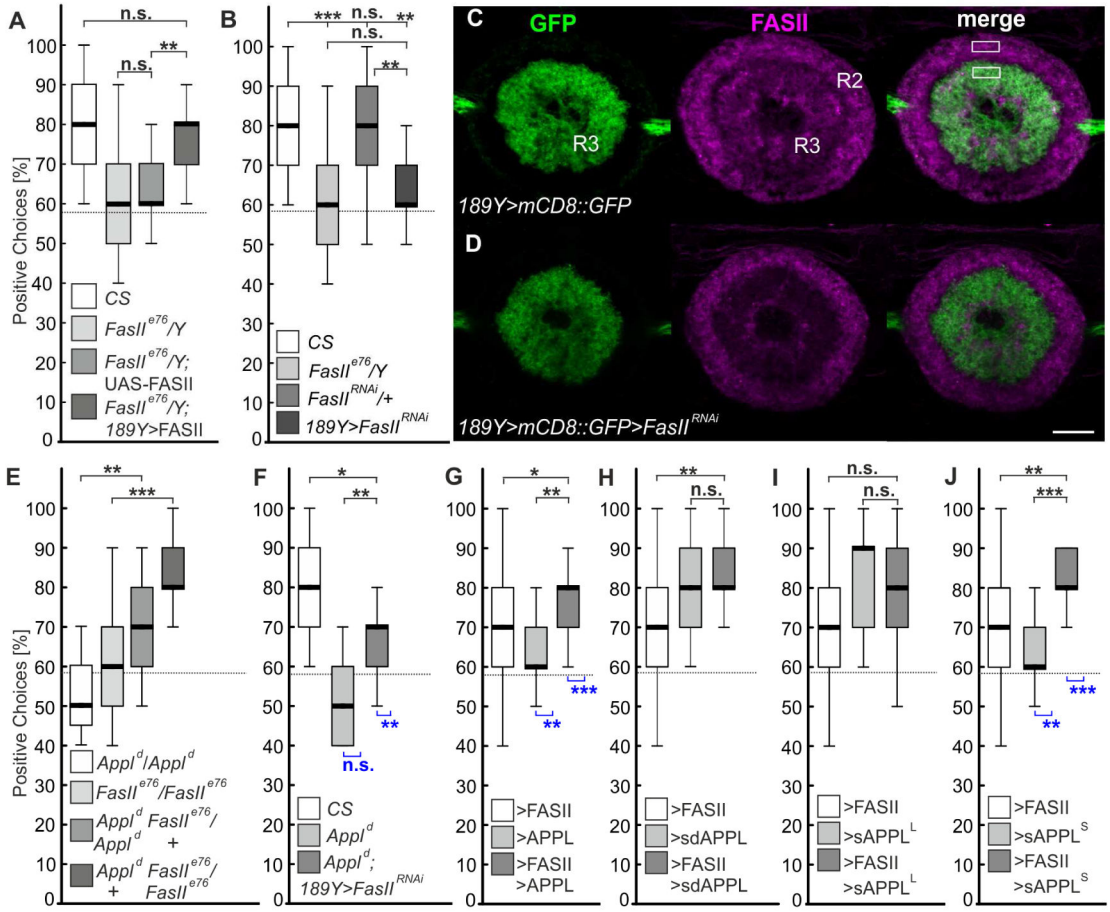

Figure 4. APPL inhibits FASII function in R3 neurons

(A) The memory deficit of hemizygous *FasII*^{e76} mutants can be rescued by FASII expression in R3 neurons, but not by the UAS-FASII transgene alone.

(B) An RNAi mediated knock-down of FASII in R3 neuron also results in memory deficit.

(C–D) Knock-down of *FasII* in R3 neurons leads to a 38% reduction of FASII levels. Rectangles indicate regions in which the means of gray value were determined to calculate the quotients of R3/R2 intensities (n = 6; p = <0.001; t-test; mean intensity ratio R3/R2: WT: 0.828 ± 0.1107; RNAi: 0.517 ± 0.0507).

(E) Heterozygosity for *Appl* or *FasII* suppresses memory deficits of homozygous *FasII*^{e76} or *Appl*^{d} mutants, respectively.

(F) Knock-down of *FasII* in R3 neurons suppresses memory deficit in *Appl*^{d} mutants.

(G) *189Y*-GAL4 driven overexpression of FASII or APPL alone reduces the working memory, but when both were co-expressed they suppress the memory deficit of each other.

(H) Overexpression of sdAPPL does not affect memory but does suppress the FASII overexpression phenotype.

(I) sAPPL^{Long} does neither affect the memory nor suppress the FASII overexpression phenotype.

(J) Overexpression of sAPPl^{Short} abolishes the memory and prevents the FASII induced phenotype.

Author Manuscript Author Manuscript Author Manuscript Author Manuscript

The *189Y*-GAL4 driver was used in all experiments; n = 25 males for all groups, except in (E) n = 16–25 females; age 3–5d; Kruskal-Wallis ANOVA, Bonferroni post-hoc. See Data S4 for statistical analysis and Figure S4 for FASII expression analysis in all types of ring neurons.